

**THE ORIENTALE ANNULAR PYROCLASTIC DEPOSIT: THICKNESS ESTIMATES FROM CRATER EXCAVATION DEPTHS.** T. A. Gaither<sup>1</sup>, L. R. Gaddis<sup>1</sup>, J. Laura<sup>1,2</sup>. <sup>1</sup>Astrogeology Science Center, U.S. Geological Survey, Flagstaff, AZ. <sup>2</sup>Department of Geography, Arizona State University, Tempe, AZ. (tgaither@usgs.gov)

**Introduction:** The Orientale annular dark mantle deposit (DMD) is a diffuse, ring-shaped, low-albedo feature located southwest of Orientale basin (29°S, 263°E, 154-km dia.) and is distributed around an elongate depression near the ring's center (**Figure 1**) [e.g., 1]. Here we present an updated estimate of the thickness of the DMD based on new high-resolution images and derived topographic products. Thickness estimates are based on the transient crater excavation depths of small, fresh lunar craters and the presence or absence of high-albedo highlands ejecta. The goal is to examine the horizontal and vertical distribution of volcanic materials and to assess the influence of local topography on deposit thickness. These results build on our initial report [2] with new imaging data that allow us to improve the identification of high-albedo highlands ejecta and the accuracy of our thickness estimates.

**Background:** Schultz and Spudis [3] interpreted the Orientale DMD and its circular nature as the result of many individual pyroclastic deposits, produced by vents that marked the location of a pre-Orientale, 175-km-diameter impact crater. Weitz et al. [4] and Head et al. [1] used Clementine UV/VIS data to interpret the central depression as the source vent, and the annular pyroclastic deposit was modeled [1, 5] as having been produced as an individual, ~2-m-thick deposit from a single, centralized vent. In this model, the Orientale DMD represents a 77-km annular deposit of sub-mm particles formed around an elongate, 7.5x16-km fissure vent, and the plume likely resembled the umbrella-shaped plumes seen on Io [e.g., 6].

**Methods:** We used imaging data from the Kaguya Terrain Camera (TC; ~10 m/pixel, [7]), Kaguya Multiband Imager (MI; ~20 m/pixel, [8]), the LRO Narrow Angle (NAC; 0.5 to 2.0 m/pixel) and Wide Angle Cameras (WAC; ~100 m/pixel, [9]), WAC stereo-derived topography [10], and MI color-ratio data [8] to characterize the geology of the DMD and to identify and measure diameters of small (<1 km dia.) lunar craters within the Orientale DMD. ArcScene 3D views of NAC frames draped over the LRO WAC DTM were also used to evaluate topography and aided our selection of craters. When examined in detail, the pyroclastic materials are seen as highly uneven in distribution, with irregular, patchy dark deposits often superimposed on low, bright hummocks and collected in shallow depressions. Nevertheless, pyroclastic deposit thickness was constrained using the depth of

excavation ( $D_{exc}$ ) of small craters according to the equations of Melosh [11], where  $D_t$  is the transient diameter,  $D_{rim}$  is the rim diameter, and  $H_t$  is the transient crater depth:  $D_t = 0.84 * D_{rim}$  and  $H_{exc} \approx 1/3 H_t \approx 1/10 D_t$ . Crater measurements were obtained in 8 regions of the DMD. These regions were selected because of their uniformly dark albedo compared to areas where there is greater relief in the underlying topography. Areas were selected for analysis based on their flat topography and a lack of hummocky terrain; in such rough areas, mantle deposits may have eroded downslope [1] and are therefore artificially thin, exposing underlying bright highlands material. Rim-to-rim diameters of 127 small craters were measured using the ArcGIS add-in Crater Helper Tools [12].

Three measurements were made for each crater (N/S, E/W, and SW/NE) and the average diameter was used to calculate the transient crater depth. Average crater diameter for the 127 measured craters is 82 m (median is 62 m) and the range is 26 to 720 m. In addition, craters were classified as “non-penetrating” (i.e., the crater did not penetrate deep enough to excavate through the DMD to expose the underlying bright-albedo highlands material) or “penetrating” (i.e., the crater did penetrate deep enough to excavate through the DMD to expose the underlying highlands material). The thickness of the DMD can be constrained to a depth between the deepest non-penetrating crater depth and the shallowest penetrating crater depth. In areas where there are no or few penetrating craters,  $D_{exc}$  of non-penetrating craters still provides a minimum thickness.

**Results:** **Figure 2** shows the Orientale DMD, with the eight regions outlined in white. Yellow and pink circles represent the measured craters (penetrating and non-penetrating, respectively). Measured values for the deepest non-penetrating craters in each of the eight regions give the most meaningful constraints on maximum thickness of the DMD, while measured values for shallowest penetrating craters highlight the variability of the underlying topography. Measurements for shallowest penetrating craters in the lowest relief areas strongly indicate the influence of topography on the resulting morphology and thickness of the deposit. Measurements for Region 1 suggest that the pyroclastic deposit is thinnest here (3.2-6.9 m), while Regions 5 and 6 have the thickest portions of the deposit (8.9-15.0 m and 4.1-17.2 m, respectively). The

range of maximum measured  $D_{exc}$  for non-penetrating craters in the eight regions is from 6.9 m to 17.2 m, with an average of 10.9 m; thus the DMD may be up to ~8 times thicker than previous estimates [1].

**Discussion.** The lunar surface beneath the Orientale DMD can be characterized as having two major layers: the megaregolith (the oldest, coarsest material, mostly large Orientale ejecta blocks of highlands material; up to ~2 km thick [13, 14]), and the overlying regolith (a thin layer of fine-grained, unconsolidated, fragmental debris of low cohesion that has formed and evolved over a long period of time from pulverization of the surface by repeated impact [15, 16]). The regolith is likely to be locally variable in thickness and may have an indistinct boundary with the underlying megaregolith [15]. Bart et al. [15] showed that the median regolith depths in various locations around the Moon are less than 10 m, with the median for Mare Orientale of 4.5 m (but perhaps higher values for typical highlands would be more appropriate to the DMD). Assuming that a ‘typical’ regolith lies beneath the dark mantle of pyroclastics and that there is likely some admixture of regolith and pyroclastic material, then thickness estimates obtained here are for a combined layer of dark, space-weathered regolith plus a dark mantle of pyroclastics. If the average thickness value of the regolith (4.5 m) is subtracted from the maximum DMD thickness values ( $D_{exc}$  of deepest non-penetrating craters), the DMD may be up to ~12 m thick in some locations.

**Summary:** The irregular distribution of dark

material suggests that the eruption may have been discontinuous and the pyroclastic material clotted and irregular (rather than a simple umbrella plume). Topography at both regional and local scales likely played a significant role in the observed DMD distribution [5]. Nevertheless our results support a likely origin of the Orientale DMD as a single eruption from a fissure vent, and suggest that the thickness of the Orientale DMD is up to ~6 times greater than previous estimates [1].

**Acknowledgements:** This work is supported by NASA through the Planetary Geology and Geophysics program. We thank the Japanese (JAXA) SELENE/Kaguya TC and MI instrument teams and the mission data archive for providing the data used here.

**References:** [1] Head et al. (2002) *J. Geophys. Res.*, 107, E1. [2] Gaither et al. (2013) *LPSC 44* abs. #2125. [3] Schultz and Spudis (1978) *Lunar Planet. Sci.*, 9, 1033-1035. [4] Weitz et al. (1998) *J. Geophys. Res.*, 103, E10, 22,725-22,759. [5] Gaddis et al. (2013) *LPSC 44* abs #2587. [6] Strom and Schneider (1982) *Satellites of Jupiter*, pp. 598-633. [7] Haruyama et al. (2008) *Adv. Sp. Res.* 42, 310-316. [8] Ohtake et al. (2010) *Space Sci. Rev.* 154, 57-77. [9] Robinson et al. (2010) *Space Sci. Rev.* 150, 81-124. [10] Scholten et al. (2012) *JGR*, v. 117, E12. [11] Melosh (1989) *Impact Cratering, A Geologic Process*. 245 pp. Oxford Press. [12] Nava (2011) Crater Helper Tools for ArcGIS10, [http://webgis.wr.usgs.gov/pigwad/tutorials/CraterHelperToolsforArcGIS%2010\\_Reference%20Manual\\_062811.pdf](http://webgis.wr.usgs.gov/pigwad/tutorials/CraterHelperToolsforArcGIS%2010_Reference%20Manual_062811.pdf). [13] Hartmann (1973) *Icarus*, 18, 634-636. [14] Thompson et al. (1979) *Moon Planets*, 21, 319-342. [15] Bart et al. (2011) *Icarus*, 215, 485-490. [16] Shoemaker et al. (1969) *J. Geophys. Res.*, 74 (25), 6081.

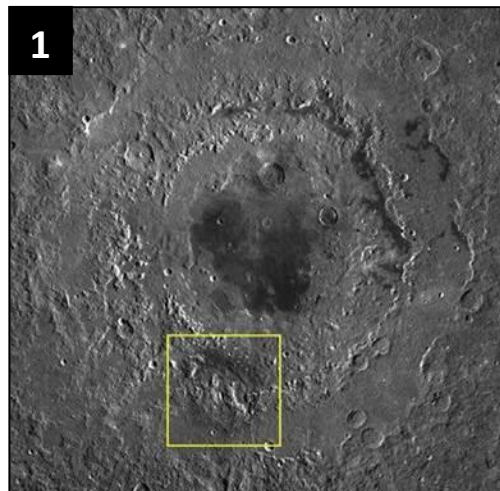


**Figure 1.** WAC mosaic centered on the DMD southwest of Orientale basin.

**Figure 2.** Overview of the distribution of measured craters in eight regions of the DMD, showing emphasis on northern portion of the annular deposit. The elongate depression in Region 9 is most probably the source vent for the DMD.

